JOURNAL OF MATERIALS SCIENCE **34** (1999) 2865–2873

Characterization of hydroxyapatite powders prepared by ultrasonic spray-pyrolysis technique

M. AIZAWA, T. HANAZAWA, K. ITATANI, F. S. HOWELL, A. KISHIOKA
Department of Chemistry, Faculty of Science and Engineering, Sophia University, 7-1, Kioicho, Chiyoda-ku, Tokyo 102, Japan
E-mail: mamaru-a@hoffman.cc.sophia.ac.jp

The hydroxyapatite (HAp) powder was prepared by the ultrasonic spray-pyrolysis technique; the characterization of the resulting powders was performed. Five kinds of the starting solutions with the Ca/P ratio of 1.67 were prepared by mixing $Ca(NO_3)_2$, $(NH_4)_2HPO_4$ and HNO_3; the concentrations of Ca^{2+} and PO_4^{3-} were in the ranges of 0.10 to 0.90 mol $\cdot$ dm^{-3} and 0.06 to 0.54 mol $\cdot$ dm^{-3}, respectively. These solutions were sprayed into the heating zone to prepare the HAp powders. The heating zone was composed of two electric furnaces; the lower furnace was used for the evaporation of the solvent from the droplets (300–500 °C) and the upper furnace for the pyrolysis of the precipitated metal salts (750–900 °C). The easily sinterable HAp powder was prepared by spray-pyrolysing the solution with Ca^{2+} (0.50 mol $\cdot$ dm^{-3}) and PO_4^{3-} (0.30 mol $\cdot$ dm^{-3}) at the temperatures of 800 °C (the upper furnaces) and 400 °C (the lower furnaces). The resulting powder was composed of the spherical particles with diameters of $\sim$1 μm or below. Even without the calcination and grinding operations, the relative densities of the compacts fired at 1150 and 1200 °C for 5 h attained maxima $\sim$95%. The microstructure of the sintered compacts appeared to be uniform; the average grain size was $\sim$3 μm. The activation energies for the grain growth of the sintered HAp compacts were 120 to 147 kJ $\cdot$ mol^{-1} $\cdot$ K^{-1}. © *1999 Kluwer Academic Publishers*

1. Introduction

The hydroxyapatite ($Ca_{10}(PO_4)_6(OH)_2$; HAp) is an inorganic compound whose composition is close to the compositions of the human hard tissues, such as the living bone and teeth. When the HAp ceramics are implanted in a body, a carbonate-containing hydroxyapatite forms on their surfaces and contributes to bonding to the living bone [1]. Thus the HAp is expected to be available as substitute materials for the human hard tissues [2, 3]. Beside such biomaterials, the HAp is applicable to the fields of ion exchangers for the harmful ions [4], adsorbents for chromatography [5], the solid ionics [6] and catalysts [7].

The techniques for the preparation of HAp powder may be classified into two [8]; one is a dry process or the solid-state reaction between calcium salts and phosphates under a steam atmosphere; the other is a wet process or the liquid-phase reaction between calcium ions and phosphate ions under alkaline conditions. The dry process is effective for the preparation of stoichiometric apatite powder; however, due to the presence of the hard agglomerates with undetermined shapes, the resulting powder shows poor sinterability. On the other hand, the HAp powder obtained by the wet process tends to form the nonstoichiometric apatite or the calcium-deficient HAp powder when the conditions for HAp preparations are not strictly controlled, regardless of the excellent sinterability of the resulting powders.

A spray-pyrolysis technique is one of the powder-preparation techniques via the liquid phases [9, 10]. This technique has advantages because one can prepare the stoichiometoric and homogeneous compounds instantaneously by spraying the solutions with the desired amounts of cations into the hot zone of an electric furnace. This technique is especially effective for the preparation of HAp-like materials containing the hydroxyl group in a crystalline structure, because the powder is directly prepared in a steam atmosphere during spray-pyrolysis [11–13].

Previous preparation of calcium phosphates with various Ca/P ratios, e.g., HAp [11, 14], tricalcium phosphate ($Ca_3(PO_4)_2$; TCP) [15, 16], calcium diphosphate ($Ca_2P_2O_7$) [15, 17] and calcium metaphosphate ($Ca(PO_3)_2$) [15, 17] by the spray-pyrolysis technique was referred. The effects of the kinds of the starting materials on properties of HAp powders prepared by spray-pyrolysis technique were also examined [14]; the stoichiometric HAp was easily prepared from $Ca(NO_3)_2$ as a calcium source and $(NH_4)_2$ HPO_4 or H_3PO_4 as a phosphorus source. Although the above experiments were carried out using a two-fluid nozzle as an atomizer, the spherical hollow particles with the diameters of $\sim$5 μm still remain [18]; thus calcination and grinding

operations were needed to produce dense HAp ceramics from the above mentioned powders [19].

Such calcination and grinding operations may be omitted when secondary particles amounted to the closely packed primary particles are formed by the spray-pyrolysis of partially polymerized metal alkoxide solution [20, 21]. Successful fracture of the spherical hollow particles was achieved by spray-pyrolysing the solutions with urea as a foaming agent [22]. The resulting powder was composed of fine particles, leading to dense sintered compacts. The crystalline phase of the powder, however, included not only HAp but also carbonate-containing HAp, because the CO_2 gas derived from the urea was introduced into the apatite structure. Thus the spray-pyrolysis using urea as a foaming agent may not be effective to prepare pure HAp but only to reduce the number of hollow agglomerates.

In order to prepare pure and easily-sinterable HAp powder without using such urea, a reduction of the droplet size was tried, by replacing the ultrasonic vibrator with two-fluid nozzle as an atomizer. Since the sizes of the particles formed in the spray-pyrolysis are dependent upon the droplet sizes [18], the reduction of the droplet size makes the formation of fine HAp particles possible. It is expected that such reduction in the droplet size may contribute to decreasing the hollow agglomerates sizes, thereby enhancing the sinterability. The purposes of the present investigation were to determine the ultrasonic spray-pyrolysis conditions for preparing the carbonate-free HAp with the stoichiometric Ca/P ratio and to examine optimum powder properties to obtain dense ceramics.

2. Experimental

2.1. Preparation of the hydroxyapatite powders

Fig. 1 shows the overall view of the ultrasonic spray-pyrolysis apparatus. The apparatus was composed of an atomizer (ultrasonic vibrator with frequency of 2.4 MHz), a heating zone (fused silica tube: I.D. 2.5 cm and height 1 m; electric furnace: I.D. 3 cm and height 60 cm) and a powder collecting zone (test-tube type filter). The hot zone in this apparatus had two electric furnaces; the lower furnace was used for the evaporation of the solvent from the droplets and the upper furnace for the pyrolysis. The aspirator was used to help collecting the powders at the suction rate of 2 $dm^3 \cdot min^{-1}$.

Five kinds of starting solutions with the Ca/P ratio of 1.67 were prepared by mixing $Ca(NO_3)_2$, $(NH_4)_2HPO_4$ and HNO_3. Table I shows the compositions of the starting solutions and the spray-pyrolysis temperatures. samples Nos. 1–6 indicate the experiments to determine the spray-pyrolysis temperatures in upper and lower furnaces, while samples Nos. 2, 7–10 are referred to the experiments for examining the effects of the concentrations in the starting solutions on some properties of the HAp powders. These solutions were sprayed into the heating zone to prepare the HAp powders. About 0.5 to 3.5 g of the powders were obtained by spraying the starting solutions with various concentrations of Ca^{2+} and PO_4^{3-} for 5 h; the total yields of powders were in the range of 70–85%.

TABLE I The composition of the starting solutions and spray-pyrolysis temperatures

Sample no.	$Ca(NO_3)_2$ ($mol \cdot dm^{-3}$)	$(NH_4)_2HPO_4$ ($mol \cdot dm^{-3}$)	Temperature (°C)	
			Upper	Lower
1	Ca/P = 1.67	0.50	0.30	900	400
2		0.50	0.30	850	400
3		0.50	0.30	800	400
4		0.50	0.30	750	400
5		0.50	0.30	850	300
6		0.50	0.30	850	500
7		0.90	0.54	850	400
8		0.70	0.42	850	400
9		0.30	0.18	850	400
10		0.10	0.06	850	400

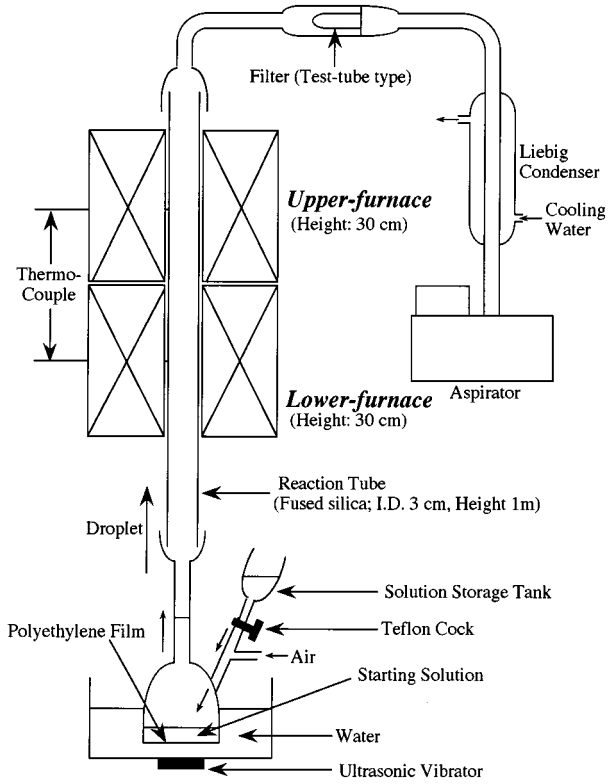

Figure 1 Overall view of the ultrasonic spray-pyrolysis apparatus.

2.2. Characterization of the resulting powders

The crystalline phases of the obtained powders were identified using an X-ray powder diffractometer (XRD) with Ni-filtered CuK_α radiation (40 kV, 25 mA), (RAD-IIA, Rigaku Corp.); the crystalline phases were checked with reference to the JCPDS cards. The lattice constants were also calculated by the least-squares method on the basis of XRD data, using (002), (210), (300), (310), (222), (213), (410) and (400) reflections of HAp. The amounts of Ca and P in each powder were determined using an X-ray fluorescence spectrometer (40 kV, 70 mA; SXF-1200, Shimadzu). FT-IR measurements were carried out by the KBr method in the ranges of 400–4000 cm^{-1} (8200D, Shimadzu). The particle shapes were observed using a scanning electron microscope (SEM; S-4500, Hitachi) and a transmission electron microscope (TEM; H-9000, Hitachi). The samples for SEM observation were prepared by setting a powder

on a carbon tape and then coating Pt-Pd on the powder. In the case of TEM observation, samples were prepared by putting powder to the micro-grids.

The specific surface area (S) was measured by the BET method using N_2 as an adsorption gas. The primary particle size (G_{BET}) was calculated by assuming the primary particles to be spherical:

$$G_{BET} = \frac{6}{\rho \cdot S}$$

where ρ is the theoretical density (3.16 $g \cdot cm^{-3}$) of HAp.

2.3. Sinterability of the resulting powders

The shrinkage of the compressed powders was measured using a thermomechanical analyzer (TMA; high-temperature type, Rigaku Denki) from R.T. up to 1300 °C at the heating rate of 10 °C · min^{-1}; the as-prepared powder was pressed at 140 MPa to form a cylindrical compact with a diameter of 5 mm and a thickness of ∼3 mm.

About 0.3 g of the as-prepared powder was uniaxially pressed at 100 MPa and then cold-isostatically pressed at 150 MPa to form the cylindrical compacts with diameters of 10 mm and heights of ∼3 mm; the compacts were fired at 1050, 1100, 1150 and 1200 °C for 5 h: the heating rate from R.T. up to the desired temperatures was 10 °C · min^{-1}.

The relative density was calculated by dividing the bulk density of the sintered compact by the theoretical density (3.16 $g \cdot cm^{-3}$) of HAp. The microstructure of the sintered compact was observed using a SEM; the grain sizes were calculated by the intercept method using SEM micrographs.

3. Results and discussion

3.1. Determination of the spray-pyrolysis conditions for HAp preparation

The sample powders in Nos. 1–6 were prepared to determine the optimum spray-pyrolysis conditions for the preparation of easily-sinterable powder. Fig. 2 shows the typical XRD pattern (a) and FT-IR spectrum (b) of the powder derived from sample No. 2. This XRD pattern showed that the crystalline phases of the resulting powder were HAp and small amount of β-tricalcium phosphate (β-TCP), although it is difficult to distinguish the overlapped reflections of HAp with those of β-TCP, due to the low crystallinities and appearance of the β-TCP reflections in the neighborhood of HAp reflections. In the FT-IR spectrum, the absorptions assigned to the PO_4 group [23] were detected at 1300–900, 600 and 570 cm^{-1} and that assigned to the OH group [24] was detected at 3570 cm^{-1}. The absorptions in the range of 1600 to 1300 cm^{-1} were assigned to the NO_3^- group [25]. In addition, the absorptions assigned to the carbonate ion were not detected in the ranges (∼1450–1550 cm^{-1}), as reported by Monma and Takahashi [26]. This IR spectrum suggests that carbonate-free HAp powder may be easily prepared by ultrasonic spray-pyrolysis technique.

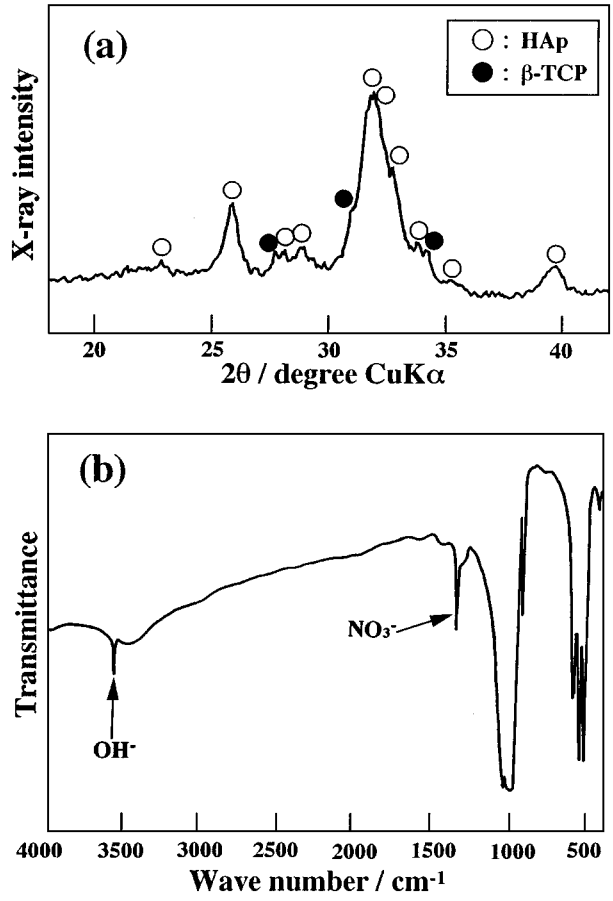

Figure 2 Typical XRD pattern (a) and FT-IR spectrum (b) of the HAp powder derived from the sample No. 2.

The crystallinity of the HAp in the present powder is higher than that of the powder prepared by spray-pyrolysis technique using the two-fluid nozzle [11, 14]. In addition, the β-TCP content in the present powder is lower than in the case of the two-fluid nozzle powder. Since the average droplet diameters formed by the two-fluid nozzle and ultrasonic vibrator are found from calculation to be ∼5 and ∼1 μm, respectively, the enhancement of the crystallinity of HAp is attributable not only to an increase in the pyrolysis temperature from 600 to 850 °C but also to the reduction of the droplet size from ∼5 to ∼1 μm.

The XRF results of the HAp powder derived from sample No. 2 showed that the Ca and P contents in the powder were 40.67 and 18.80 mass%, respectively. The Ca/P molar ratio was found from calculation to be 1.67, which agrees well with that of a stoichiometric composition of the HAp. Lattice constants (a- and c-axes) of this HAp powder were measured; the lattice constants of a- and c-axes were 0.9434 and 0.6883 nm, respectively. The present constants are close to the reported lattice constants of a-axis (0.9432 nm) and c-axis (0.6881 nm) [26]. The results of XRF and lattice constants revealed that the present HAp powder obtained by the ultrasonic spray-pyrolysis has a high purity and stoichiometric composition.

The XRD patterns and FT-IR spectra of other sample powders were almost the same as those of the sample powder No. 2. The results were summarized as follows: β-TCP in the powders was present when

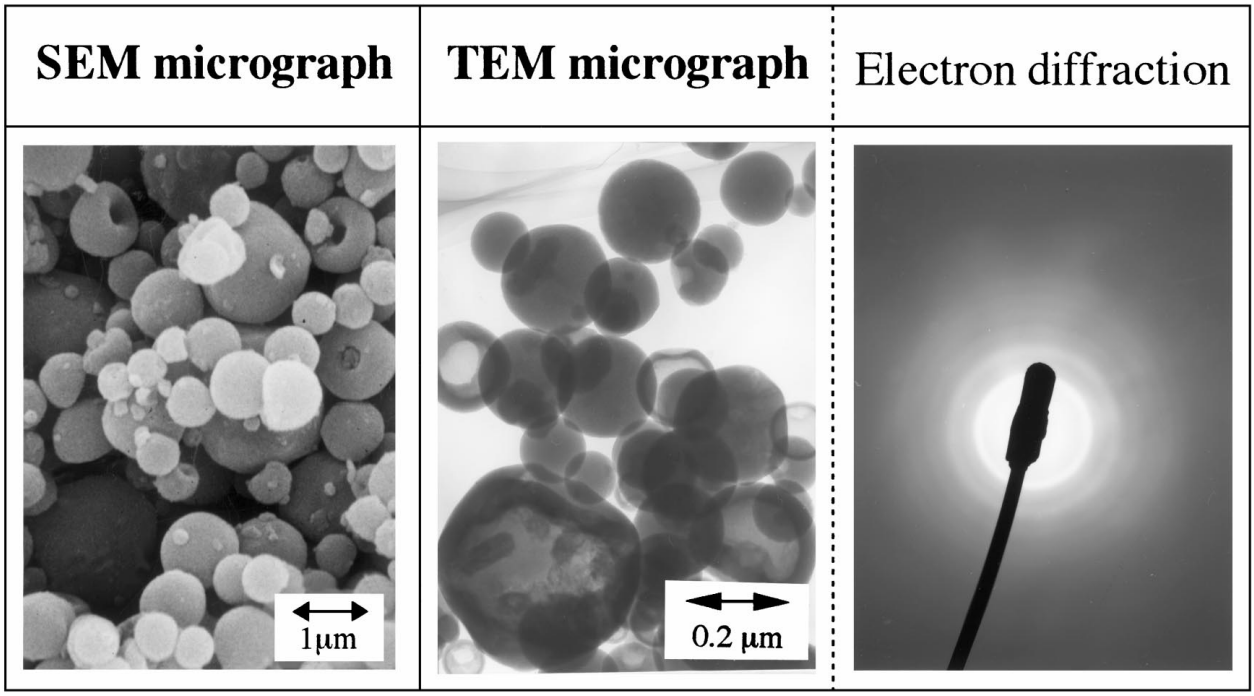

Figure 3 SEM and TEM micrographs of the HAp powder derived from the sample No. 2, together with the electron diffraction image of the TEM micrograph.

the upper-furnace temperature was below 850 °C; only HAp was present when the upper-furnace temperature was raised up to 900 °C; crystallinity of the resulting HAp powder was enhanced with an increase of the upper- and lower-furnace temperatures.

HAp particles for sample powders Nos. 1 to 6 were observed using SEM and TEM. The particles morphologies of sample powders 1 to 6 were similar to one another. Typical results of sample powder No. 2 are shown in Fig. 3, together with the electron diffraction image. The SEM micrograph indicated that the resulting HAp powder was composed of spherical particles with the diameters of ∼1 μm or below. The TEM micrograph showed that inside some spherical particles were translucent. This observation suggests that the resulting powder is partly composed of the spherical and hollow particles. Since the particle sizes in the case of the two-fluid nozzle were ∼5 μm [11, 14], it is noteworthy that by using ultrasonic spray-pyrolysis, the particle sizes are reduced down to one fifth. The electron diffraction image showed the ring patterns with the concentric circles. Taking the XRD patterns of the resulting powders into account, these diffraction rings may be ascribed to those of HAp. Since that distinct spots did not appear in the electron diffraction image, the particles seem to be composed the minute polycrystals.

In order to examine the densification behaviour of the resulting HAp powders during heating, the linear shrinkage of the compact was measured using TMA. Fig. 4 shows the results of the typical powder compact of sample 2. In the shrinkage curve ($\Delta L/L$), the shrinkage of the compact initiated at ∼650 °C; it increased with temperature and attained ∼16% at 1300 °C. In the derivative curve (d($\Delta L/L$)), the shrinkage rate was divided into two regions: i.e., (i) 700–800 °C and (ii) 1050–1200 °C.

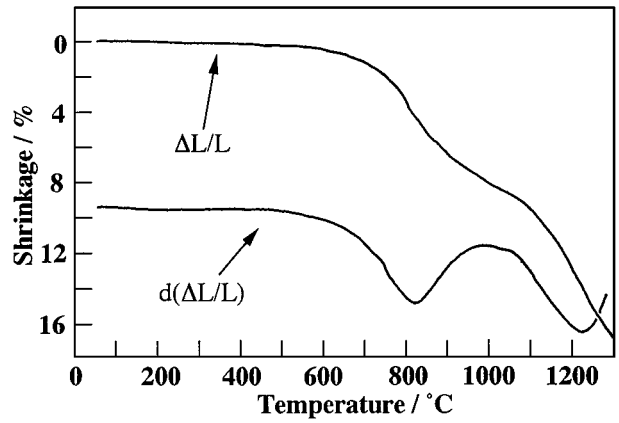

Figure 4 Linear shrinkage curve and shrinkage-rate curve of the HAp compact of the sample No. 2 at the heating rate of 10 °C · min^{-1}.

The shrinkage behaviour of the HAp compact is divided into two stages. In the range of (i) 700–800 °C, the shrinkage of the HAp compact may be due to the sintering of the primary particles within the spherical and hollow secondary particles [19]. In the range (ii) 1050–1200 °C, the shrinkage appears to occur due to the sintering of the secondary particles/grains [19].

On the basis of the above results and previous reports [11, 13, 14, 22], the sinterability of the compressed powders 1 to 6 at 1150 °C for 5 h was examined. Fig. 5a shows the results on the changes of the relative density with increasing the upper-furnace temperature; the lower-furnace temperature was fixed to be 400 °C. Fig. 5b indicates the results on the effects of the relative density with increasing the lower-furnace temperature; the upper-furnace temperature was fixed to be 850 °C. The relative density of the sintered compact attained a maximum (∼95%) when the furnace temperatures were fixed to be 850 °C (upper furnace) and 400 °C (lower

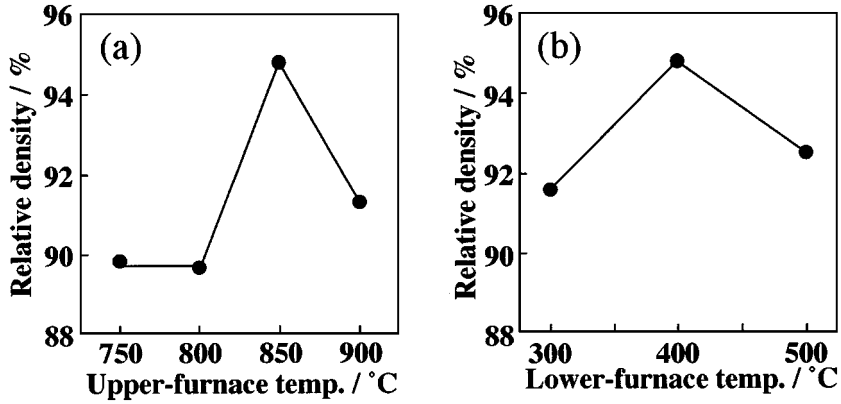

Figure 5 Changes of the relative density with increasing (a) lower-, and (b) upper-furnace temperatures (Sample Nos. 1 to 6). Firing conditions, 1150 °C, 5 h. (a) Lower-furnace temperature of 400 °C. (b) Upper-furnace temperature of 850 °C.

furnace). The powder derived from sample No. 2 shows the best sinterability among the powders 1–6. The XRD patterns were omitted in this paper, because they were almost the same as those for Fig. 9 described in the later section. The results obtained were summarized as follows: (1) the crystalline phase of the above sintered compacts was only HAp, (2) the absorptions assigned to the NO_3^- group disappeared.

Taking the spray-pyrolysis temperatures for preparing the easily-sinterable HAp powder into account, we determined the spray-pyrolysis temperature to be 850 °C for upper-furnace and 400 °C for lower-furnace. Although calcination and grinding operations are needed to fabricate the dense HAp ceramics from the powders prepared using the two-fluid nozzle [19], they may be omitted when the present HAp powder, prepared using the ultrasonic vibrator, is used for the fabrication of the HAp ceramics. We conclude that the ultrasonic spray-pyrolysis technique is effective for preparing the easily-sinterable HAp powder.

3.2. Effect of the concentration of the starting solution on the properties of the HAp powder

The effect of the concentration of the starting solution on the formation and properties of the HAp powder was examined by fixing the spray-pyrolysis temperature to be 850 °C (upper-furnace) and 400 °C (lower-furnace) (Samples 2, 7–10).

The main crystalline phase of the powder obtained from samples 2 and 7–10 was HAp; however, a small amount of β-TCP was present in the case of samples 7 and 8. The FT-IR results showed that these spectra included the absorption peak of $\sim$3570 cm^{-1} or the peak characteristic of HAp. The obtained powders were observed by SEM; typical micrographs are shown in Fig. 6. These SEM micrographs indicated that the resulting powders were composed of spherical particles with diameters below 2 μm. These particle diameters were reduced with decreasing concentration of the starting solution.

The spherical particles may be formed via the following processes [13, 18]: (i) the removal of the solvent from the droplet surface, (ii) the formation of microcrystalline calcium phosphates and (iii) the crystal growth of calcium phosphates. The resulting spherical particle diameters are dependent upon the droplet sizes of the starting solution. The droplet size may be reduced with decreasing concentration of the starting solution, thus reducing the spherical particle diameters.

Fig. 7 shows the relationship between specific surface area (SSA) and concentration of the starting solution. The SSA decreased with an increase of the starting solution concentration; the SSA of the sample No. 10 was the largest ($\sim$45 $m^2 \cdot g^{-1}$) among the SSAs of the powders examined. Such decrease of the SSA suggests that the growth of the primary particles may be inhibited with increasing the concentration of the starting solution. Since most of the spray-pyrolysis times were spent in removing the solvent from the droplet in the case of the dilute solutions, such as No. 10, the growth of crystals precipitated within the droplets may not be thoroughly promoted during the spray pyrolysis.

Sintered compacts were produced from the above mentioned powders and some properties of the resulting compacts were examined. Fig. 8 shows the relationship between firing temperature and relative density of the sintered compact. The relative density of the compact increased with firing temperature. In the sample powder of No. 2, the relative densities at 1150 or 1200 °C attained $\sim$95%; these values were the highest among the HAp powders examined.

As a typical example of the sample powders (No. 2), the XRD pattern of the sintered compact fired at 1200 °C for 5 h is shown in Fig. 9. The crystalline phase of the sintered compact was only HAp. The TCP phase was not detected in the sintered compact, although the calcium-deficient HAp is decomposed to form the TCP phase during firing [8]. This fact shows that the present HAp has the stoichiometric composition. FT-IR spectra did not contain any absorptions assigned to NO_3^-; only the characteristic absorptions assigned to HAp were detected from the compacts fired at 1050–1200 °C for 5 h. The XRD patterns and FT-IR spectra of Nos. 7 to 10 were almost the same as those of the sintered compact derived from the sample powder No. 2.

Fig. 10 shows typical SEM micrographs of polished surfaces of the sintered compacts derived from the sample powder No. 2. These sintered compacts were

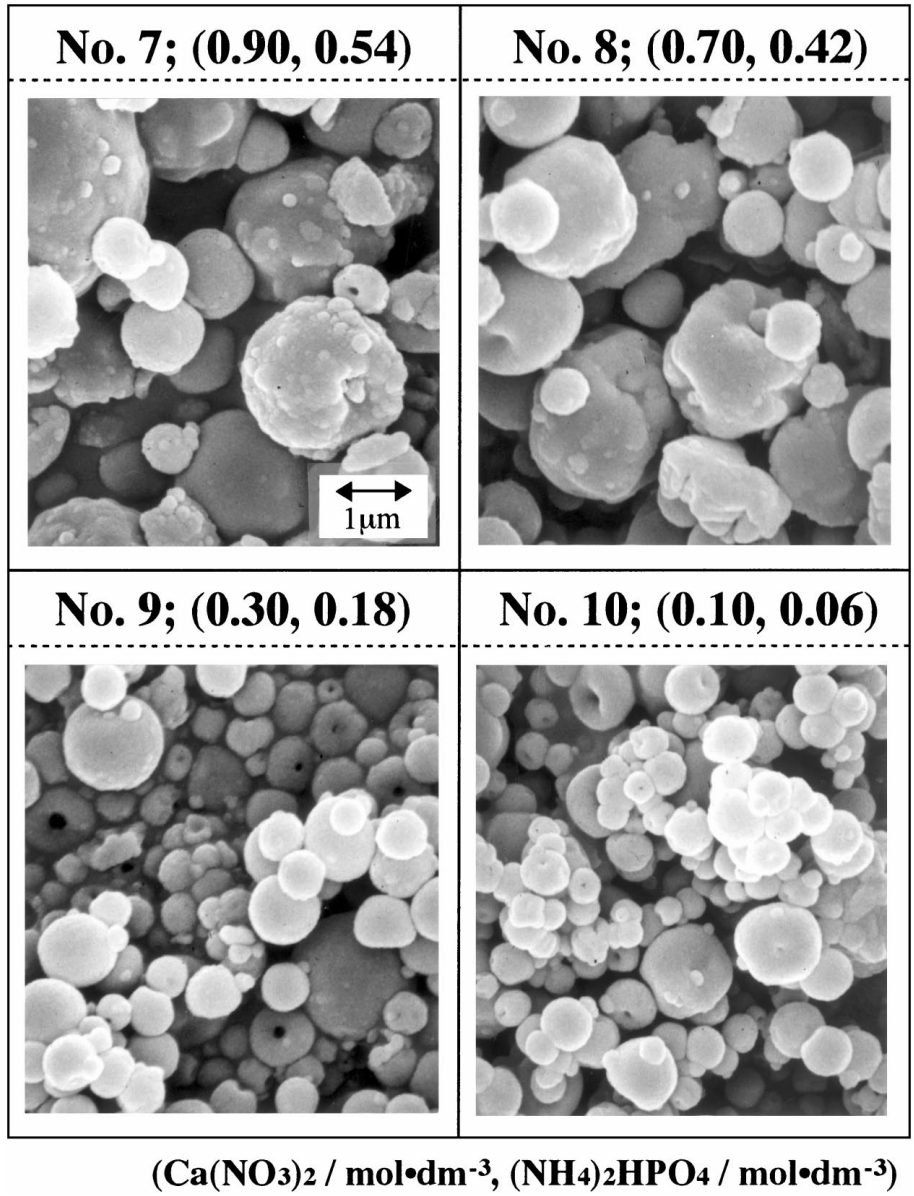

Figure 6 SEM micrographs of the HAp powders derived from the starting solutions with various Ca^{2+} and PO_4^{3-} concentrations (Sample Nos. 7 to 10).

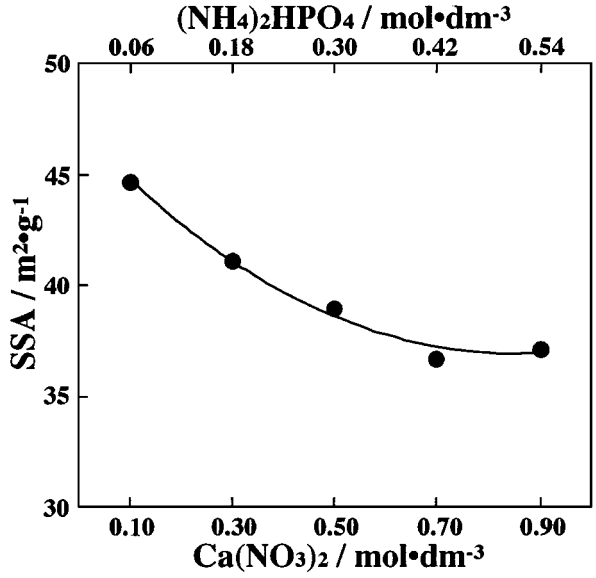

Figure 7 Relationship between concentration of the starting solution and specific surface area (Sample Nos. 2, 7 to 10).

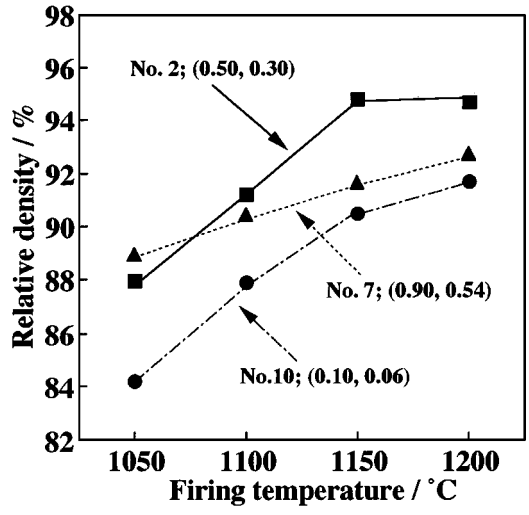

Figure 8 Relationship between firing temperature and relative density of the HAp compact derived from the various starting solutions (Firing time, 5 h; Sample Nos. 2, 7 and 10).

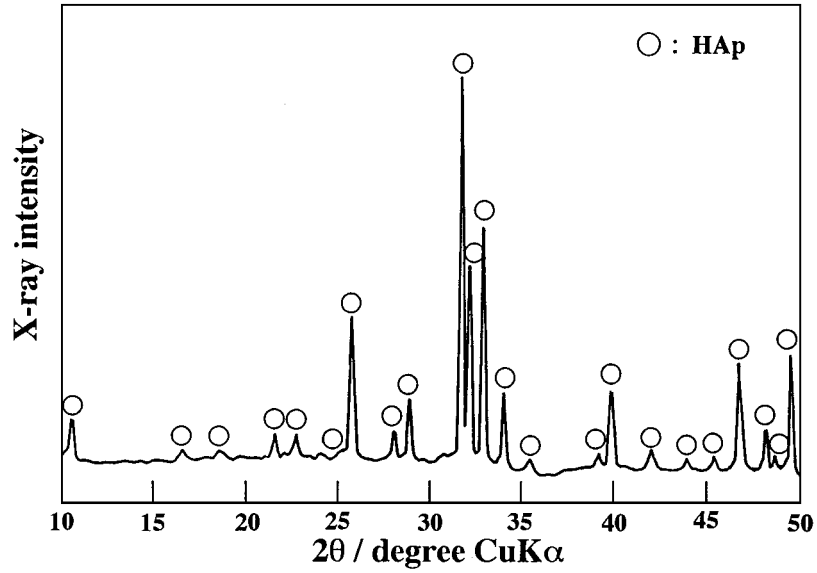

Figure 9 XRD pattern of the sintered HAp compact fired at 1200 °C for 5 h (Sample No. 2).

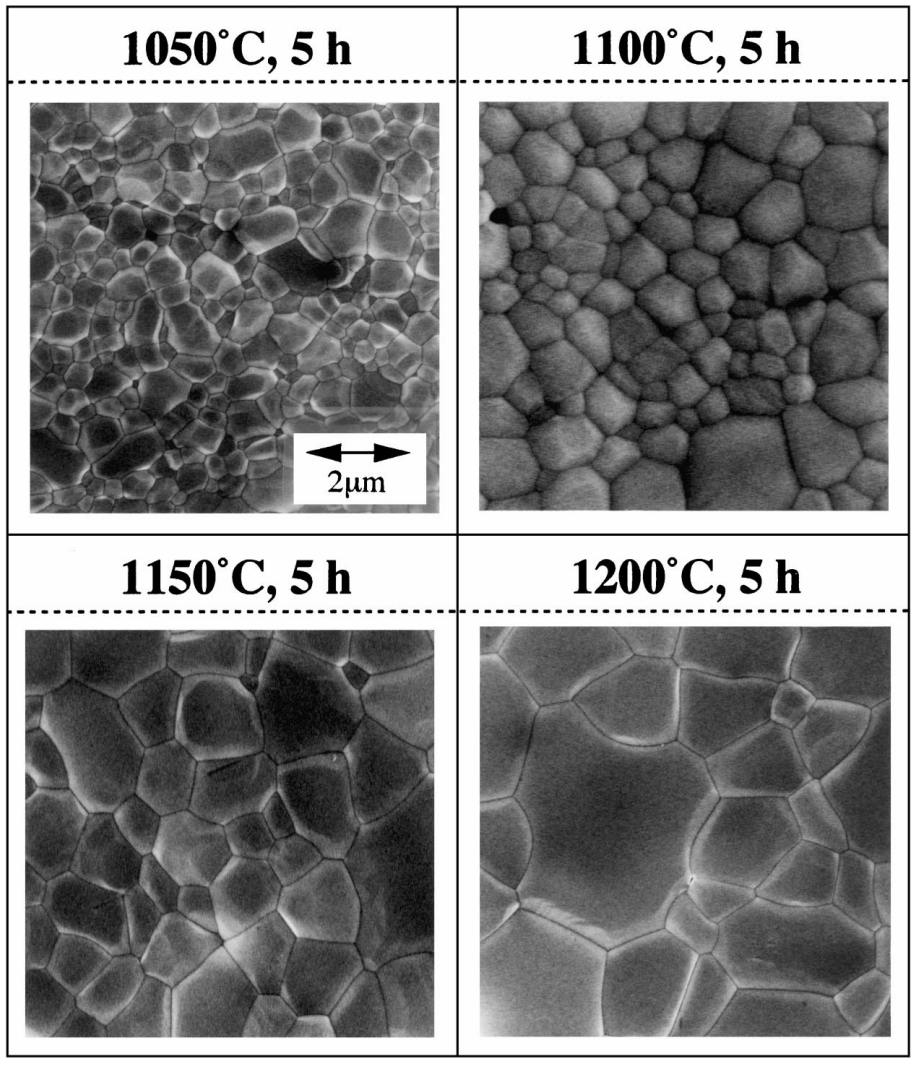

Figure 10 SEM micrographs of the sintered compacts fired at 1050, 1100, 1150 and 1200 °C for 5 h (Sample No. 2).

composed of uniform-sized grains; the grain size increased with firing temperature. The average grain size was calculated by the interception method from the micrographs of the sintered compacts. Results are shown in Fig. 11. For all specimens, the average grain size increased gradually from ∼0.7 μm to 2–3 μm with firing temperature. On the basis of the above data, the apparent activation energies for the grain growth of HAp

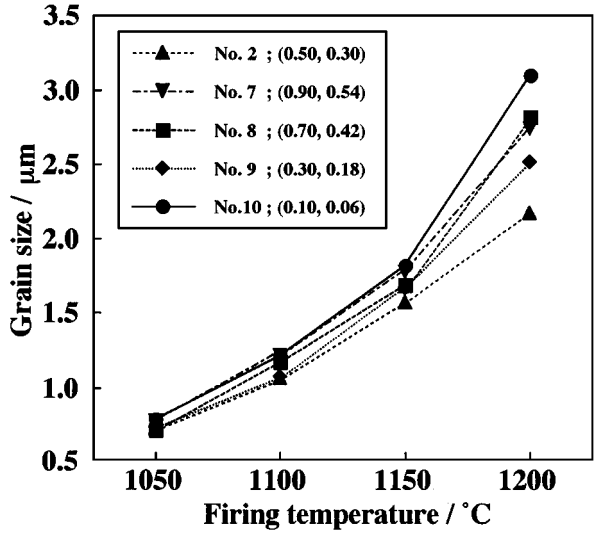

Figure 11 Relationship between firing temperatures and average grain sizes of the HAp compacts (Firing time, 5 h; Sample Nos. 2, 7–10).

were calculated from the Arrhenius plot of ln$G$ vs. $1/T$, where G is the average grain size (μm) and T is the absolute temperature (K). The activation energies calculated from the slopes of Arrhenius plots were in the range of 120 to 147 $kJ \cdot K^{-1} \cdot mol^{-1}$.

The present activation energies are in accordance with those from grain growth of HAp, $\sim$130 $kJ \cdot K^{-1} \cdot mol^{-1}$ (Kijima and Tsutsumi [27]) and $\sim$142 $kJ \cdot K^{-1} \cdot mol^{-1}$ (De With *et al.* [28]). The activation energy ($\sim$234 $kJ \cdot K^{-1} \cdot mol^{-1}$) reported by Jarcho *et al.* [29] is higher than the present energy. This activation energy was re-calculated by Ioku, who found that the corrected activation energy was $\sim$130 $kJ \cdot K^{-1} \cdot mol^{-1}$ [30]. In addition, the HAp releases a part of the OH group as H_2O at 800 °C or higher; thus sintering appears to proceed leading to the formation of oxyapatite [31], $Ca_{10}(PO_4)_6$ O □ (□:vacancy), during firing at 1050 to 1200 °C for 5 h. In order to determine the activation energy without release of the OH group in HAp, the grain growth of the HAp under the steam atmosphere has to be examined. Sintering of HAp under such conditions will soon be objective of research.

4. Conclusion

HAp powder was prepared by ultrasonic spray-pyrolysis. The results obtained are summarized as follows:

(1) The easily-sinterable HAp powder was prepared when the spray-pyrolysis temperature was 850 °C for the upper-furnace and 400 °C for the lower-furnace. The XRF results of HAp powder showed that the Ca and P contents in the powder were 40.67 and 18.80 mass%, respectively; the Ca/P ratio was found from calculation to be 1.67. The lattice constants of *a*- and *c*-axes of the HAp were 0.9434 and 0.6883 nm, respectively. The resulting powder was composed of the spherical particles with the diameters of $\sim$1 μm or less.

(2) The effect of the starting solution concentration on the formation and properties of the HAp powder was examined under the above spray-pyrolysis conditions. The crystalline phases of the resulting powders were chiefly HAp. These powders were composed of spherical particles with diameters below 2 μm; the particle diameters were reduced with decreasing concentration of the starting solution. The SSA decreased with an increase in the starting solution concentration.

(3) The sintered HAp compact with the highest relative density of $\sim$95% was obtained by firing the powder compact derived from the sample No. 2 at 1150 or 1200 °C for 5 h. The microstructure of the sintered compact was composed of uniform grains with the sizes of $\sim$3 μm. The activation energies for the grain growth of the HAp were in the range of 120 to 147 $kJ \cdot K^{-1} \cdot mol^{-1}$.

References

1. T. KOKUBO, *Biomater.* **12** (1991) 155.
2. L. L. HENCH, *J. Amer. Ceram. Soc.* **74** (1991) 1487.
3. J. WILSON, A. YLI-URPO and RISTO-PEKKA HAPPONEN, "An Introduction to Bioceramics," Vol. 1, edited by L. L. Hench and J. Wilson (World Scientific, Singapore, 1993) p. 139.
4. T. SUZUKI, *Gypsum & Lime* (204) (1986) 58.
5. T. KAWASAKI, *J. Chromatgr.* **544** (1991) 147.
6. K. YAMASHITA and T. UMEGAKI, *Inorganic Materials* **2** (1995) 166.
7. H. MONMA, *J. Catalysis* **75** (1982) 200.
8. T. KANAZAWA, T. UMEGAKI, H. MONMA and K. YAMASHITA, *Gypsum & Lime* (210) (1987) 261.
9. G. L. MESSING, S. -C. ZHANG and G. V. JAYANTHI, *J. Amer. Ceram. Soc.* **76** (1993) 2707.
10. T. SUZUKI, K. ITATANI, M. AIZAWA, F. S. HOWELL and A. KISHIOKA, *J. Euro. Ceram. Soc.* **16** (1996) 1171.
11. K. ITATANI, O. TAKAHASHI, A. KISHIOKA and M. KINOSHITA, *Gypsum & Lime* (213) (1988) 19.
12. S. INOUE and A ONO, *J. Ceram. Soc. Jpn.* **95** (1987) 759.
13. M. AIZAWA, T. HANAZAWA, K. ITATANI, F. S. HOWELL and A. KISHIOKA, *Phosphorus Res. Bull.* **6** (1996) 217.
14. M. AIZAWA, K. ITATANI, F. S. HOWELL and A. KISHIOKA, *J. Ceram. Soc. Jpn.* **104** (1996) 126.
15. K. ITATANI, M. AIZAWA, F. S. HOWELL, A. KISHIOKA and M. KINOSHITA, *Phosphorus Res. Bull.* **1** (1991) 35.
16. K. ITATANI, T. NISHIOKA, S. SEIKE, F. S. HOWELL, A. KISHIOKA and M. KINOSHITA, *J. Amer. Ceram. Soc.* **77** (1994) 801.
17. M. AIZAWA, Y. MIYAMOTO, K. ITATANI, A. KISHIOKA and M. KINOSHITA, *Gypsum & Lime* (237) (1992) 22.
18. K. ITATANI, A. KISHIOKA and M. KINOSHITA, *Gypsum & Lime* (241) (1992) 447.
19. O. TAKAHASHI, K. ITATANI, A. KISHIOKA and M. KINOSHITA, *Gypsum & Lime* (225) (1990) 19.
20. N. ISHIZAWA, O. SAKURAI, N. MIZUTANI and M. KATO, *J. Ceram. Soc. Jpn.* **93** (1985) 382.
21. K. NOGAMI, O. SAKURAI, N. MIZUTANI and M. KATO, *ibid.* **95** (1987) 682.
22. M. AIZAWA, K. ITATANI, F. S. HOWELL and A. KISHIOKA, *ibid.* **103** (1995) 1214.
23. B. O. FOWLER, E. C. MORENO and W. E. BROWN, *Arch. Oral. Biol.* **11** (1966) 477.
24. Y. ARAI and T. YASUE, *Gypsum & Lime* (187) (1983) 357.
25. H. MONMA and T. TAKAHASHI, *Gypsum & Lime* (210) (1987) 261.
26. JCPDS # 9-432.
27. T. KIJIMA and M. TSUTSUMI, *J. Amer. Ceram. Soc.* **62** (1979) 455.

28. G. DE WITH, H. J. A. VAN DIJK, N. HATTU and K. PRIJS, *J. Mater. Sci.* **16** (1981) 1592.
29. M. JARCHO, C. H. BOLEN, M. B. THOMAS, J. BOBICK, J. F. KAY and R. H. DOREMUS, *ibid.* **11** (1976) 2027.
30. K. IOKU, Doctoral Thesis, Tokyo Institute of Technology, 1990, p. 192.
31. J. C. ELLIOTT, "Structure and Chemistry of the Apatites and Other Calcium Orthophosphates" (Elsevier, Amsterdam, London, New York, Tokyo, 1994) p. 127.

Received 9 February 1998
and accepted 22 January 1999